

MRA HOMOGENIZATION UNDER ULTRA WIDEBAND (UWB) CONDITIONS AND FAULT INTERROGATION

Vitaliy Lomakin⁽¹⁾, Ben Zion Steinberg⁽²⁾ and Ehud Heyman⁽³⁾

Faculty of Engineering, Tel-Aviv University, Tel-Aviv, 69978, Israel.

E-mail: ⁽¹⁾ vitaliy@eng.tau.ac.il, ⁽²⁾ steinber@eng.tau.ac.il, ⁽³⁾ heyman@eng.tau.ac.il

ABSTRACT

The recently developed multi-resolution homogenization theory (MRH) is extended in this paper to operation under UWB/short-pulse conditions. We consider two homogenization strategies, a dispersive and a non-dispersive one, and explore their effect on the time domain modeling of the travelling-wavefronts and resonances phenomena. These time domain signatures are applied then for fault interrogation and identifications. All these results are supported by numerical tests and demonstrations.

INTRODUCTION

The study of propagation and/or scattering of EM waves in multi-scale heterogeneity laminates is of fundamental importance in diverse areas of applications such as material synthesis, circuits design, fault interrogation, etc. The most complete data base is furnished by the ultra wideband (UWB) short-pulse waves. As the scales of the laminate heterogeneity ranges from the *micro* (a fraction of a wavelength) to the *macro* (wavelength and above), the analysis of the entire set of associated wave phenomena and their detailed structure pose a problem of overwhelming complexity.

In most applications, however, the detailed (micro-scale) structure of the field is of no practical importance. This can be due to the properties of the field itself or due to the relevant observables and the measurement setup. The role of homogenization theory is to derive a physically cogent, simpler to solve, *effective formulation* for the *macro-scale field* which smoothes out the micro-scale heterogeneities while retaining their effect on the macro scale observables.

In this work we utilized the recently derived theory of multiresolution homogenization (MRH), which is a *full-wave effective theory* for *source excited* electromagnetic (and other) wave fields in three dimensional (3D) finely layered structures [1]–[4]. This theory includes all the full-wave features that enable one to construct rigorous spectral solutions for the field as well as alternative physical parameterizations in terms of rays (including diffraction effects), modes (including leaky waves), traveling wavefronts or resonances, as well as a hybrid combinations of the above. The theory utilizes a novel two scale approach in which the field and the medium are homogenized on different scales. This scheme removes the need for a large gap between the micro and the macro scales in the medium, and as such it is particularly suitable for modeling ultra wideband (multi-scale) sources and fields.

The objectives of this work is to apply the effective theory to UWB fields. We consider two alternative approaches to UWB homogenization: *dispersive* and *non-dispersive* approaches, and explore their effect on the time domain modeling of the *travelling-wavefronts* and *resonances* phenomena, including a bound on the resonance equivalence. Finally we consider an application where the MRH is used to determine the conditions for fault interrogation and detection in multi-scale heterogeneous laminate using transient fields.

PROBLEM FORMULATION

We consider a source-excited EM field in a complex laminate that resides in $0 < z < d$ surrounded by homogeneous domains at $z < 0$ and $z > d$, that has an unbounded cross section perpendicular to the z axis. The constitutive parameters are assumed to be diagonal tensors whose components $\varepsilon_z, \varepsilon_t, \mu_z, \mu_t$ (the subscripts z and t denote the z and transverse components, respectively) are *multi-scale* functions of z comprising of both macro and micro scales.

As an example, we consider an incident pulsed plane wave excited by a current sheet $\mathbf{J}(\mathbf{r}) = \hat{\mathbf{y}}J_y(t - x\xi/c, z)$, where the parameter $\xi = \sqrt{\xi\xi} < 1$ describes a linear delay along x . The resulting TM field can be found from $\mathbf{E}(\mathbf{r}, t) = \hat{\mathbf{y}}E_y(t - x\xi/c, z) + \hat{\mathbf{z}}E_z(t - x\xi/c, z)$ and $\mathbf{H}(\mathbf{r}, t) = \hat{\mathbf{x}}H_x(t - x\xi/c, z)$. Substituting into Maxwell's equations yields the transmission line equations

$$\frac{\partial}{\partial z}E_y = -c^{-1}p(z)\frac{\partial}{\partial t}H_x - J_y, \quad \frac{\partial}{\partial z}H_x = -c^{-1}q(z)\frac{\partial}{\partial t}E_y \quad (1)$$

where $p = \mu_t - \xi^2\varepsilon_z^{-1}$ and $q = \varepsilon_t$. Note that the TE field can be excited by $\mathbf{J}(\mathbf{r}) = \hat{\mathbf{y}}J_x(t - x\xi/c, z)$ and is obtained by replacements: $E_{y,z} \rightarrow H_{x,z}$, $H_x \rightarrow E_y$ and with $p = \mu_t$, $q = \varepsilon_t - \xi^2\mu_z^{-1}$.

EFFECTIVE FORMULATION

We start with summarizing the effective formulation in the frequency domain. We are mainly concerned with the large-scale components of the response. The effective formulation is therefore checked and validated on the *field homogenization scale* (F-HS) which is defined on a binary scale to be F-HS = 2^{-j} . In most cases it is determined by the *local wavenumber* in the *effective medium* (the latter will be defined in (2)).

The medium is described on a different scale, termed the *medium homogenization scale* M-HS = $2^{-\nu}$, and the error of the effective formulation depends on the scale $2^{-(\nu+1)}$ which is the maximal scale that is neglected in the homogenization. Actually, if the medium has a scale gap then the homogenized medium is described on a larger scale, say = 2^{-M} with $M < \nu$, yet the error still depends on the neglected scale $2^{-(\nu+1)}$. Thus for simplicity we consider only the more general case where M-HS = $2^{-\nu}$.

The effective formulation is given by Equation (1) but with the medium $\varepsilon_{z,t}$ and $\mu_{z,t}$ replaced with simpler *effective medium* $\varepsilon_{z,t}^{\text{ef}}$ and $\mu_{z,t}^{\text{ef}}$ given by

$$\varepsilon_t^{\text{ef}} = \mathcal{P}_\nu \varepsilon_t, \quad \varepsilon_z^{\text{ef}} = [\mathcal{P}_\nu(\varepsilon_z^{-1})]^{-1}, \quad \mu_t^{\text{ef}} = \mathcal{P}_\nu \mu_t, \quad \mu_z^{\text{ef}} = [\mathcal{P}_\nu(\mu_z^{-1})]^{-1}. \quad (2)$$

where \mathcal{P}_ν is the operator projecting the field onto smooth space (see [5]).

A measure of the accuracy of the effective formulation is given by the norm (see [2])

$$\frac{\|\mathcal{P}_j E_y - \mathcal{P}_j E_y^{\text{ef}}\|}{\|\mathcal{P}_j E_y^{\text{ef}}\|} \sim \left(\omega/cK\right)^3 2^{-2\nu} d M_\nu^2 \quad (3)$$

where d is the thickness of the slab, c is the free space wavespeed, $K = \max\{\sqrt{p^{\text{ef}} q^{\text{ef}}}\}$. The parameter $M_\nu = \|q^d\|^2 / \|q^{\text{ef}}\|^2 + \|p^d\|^2 / \|p^{\text{ef}}\|^2$ defines the ratio between the norm of the detail and smooth parts of the medium heterogeneities, where $p^d = \mathcal{P}_\nu p$, $q^d = \mathcal{P}_\nu q$ (see (2)) while $p^d = \mathcal{D}_\nu p$ and $q^d = \mathcal{D}_\nu q$, where \mathcal{D}_ν is the operator projecting onto the orthogonal complement of the smooth space (see [5]).

UWB HOMOGENIZATION SCHEMES

As discussed above and as follows from bound (3) the F-HS and M-HS are typically chosen relative to the wavelength. For ultra wideband excitations, the spectrum of the excitation pulse covers a wide range of wavelengths. This leads to two alternative homogenization strategies:

A dispersive homogenization approach: Here the source spectrum is divided into sub-bands, and the M-HS is chosen for each band so that the bound (3) is sufficiently small there. This approach provides the simplest medium for each frequency within the source operation band, yet the field equations have to be solved on a frequency-by-frequency basis.

A non-dispersive homogenization approach: Here the M-HS is chosen to comply with (3) at the highest excitation frequency and then used for the entire operation band. Clearly this approach does not provide the most economical description of the medium at each frequency, yet it allows for direct time domain solutions as the effective medium is frequency independent.

PARAMETERIZATION OF THE FIELD OBSERVABLES

The response to an UWB short pulse excitation can be parameterized via two alternative representations:

Traveling wave representation: Here the field is described as a successive arrivals of pulsed wave-fronts describing multiple reflections and interactions within the slab. To demonstrate the effect of the homogenization on this representation, we consider a complex slab with $\mu = 1$ but complex (i.e., multiscale) ε . We synthesize this medium using the wavelet functions $\psi_{mn}(z) = 2^{m/2} \psi(2^m z - n)$ (see [5]), giving $\varepsilon_t = 2(1 + \sum_n \sum_{m=4}^{10} \varepsilon_{t mn} \psi_{mn}(z))$, $\varepsilon_z = 2(1 + \sum_n \sum_{m=4}^{10} \varepsilon_{z mn} \psi_{mn}(z))^{-1}$. We generate the coefficients $\varepsilon_{t mn}$ and $\varepsilon_{z mn}$ randomly as $\varepsilon_{t mn} = 0.075 f_t(m, n) 2^{-m/2}$, $\varepsilon_{z mn} = 0.3 f_z(m, n) 2^{-m/2}$, where $f_t(m, n) = \pm 1$ and $f_z(m, n) = \pm 1$ are uniformly distributed random functions of m, n . The $\sim 2^{-m/2}$ behaviour of $\varepsilon_{t,z}$ is chosen so that their norms are evenly distributed in the scale domain m . The incident pulse is taken to be $f(t) = \frac{T}{\pi[(t-4T)^2 + T^2]}$ with $cT = 2^{-3}$, spanning frequencies from 0 up to $(cT)^{-1} \sim 16$.

The transient reflected field is shown in Fig. 1. The plot shows the reflected field for the non-dispersive approach for two values of the M-HS with $\nu = 4$ and $\nu = 6$. One observes a slight error in the effective result for the former, but an excellent accuracy (no noticeable error) for the latter.

Effective SEM resonances: The UWB field may be parameterized alternatively as in the Singularity Expansion Method (SEM) [6], in terms of oscillatory (standing wave) solutions, associated with the complex resonance frequencies source-excited field solution. The resonances describe the transient response as a series of decaying oscillations and

thus may serve for medium classification. It has been established that the SEM resonances of the effective problem (denoted ω_l^{ef} with l being an index) are equivalent to those ω_l of the actual problem, with an error bound

$$|\omega_l - \omega_l^{\text{ef}}| \sim (\omega_l^{\text{ef}})^3 K^2 c^{-2} 2^{-2\nu} M_\nu^2, \quad (4)$$

where the parameter K and M_ν are defined in (3). This equivalence defines the conditions under which the effective formulation can be used to parameterize the actual (e.g., measured) resonance observables. The equivalence between the actual and effective complex resonances and the quality of the theoretical bound (4) are demonstrated in Fig. 2 for the same medium used in the previous example, which depicts the error $|\omega_l - \omega_l^{\text{ef}}|$ on a \log_2 scale as a function of the M-HS index ν . One readily observes that the error behaves like $2^{-2\nu}$ as predicted in (4).

EFFECTIVE PARAMETERIZATION AND INTERROGATION OF 1D FAULTS

Finally, we consider an application where the MRH is used to parameterize the UWB signature of faults in the laminate. The faults considered are inclusion whose transversal size is large, so that they can be denoted as essentially one dimensional (1D) faults since, from an analysis point of view, the medium can still be considered as layered. We assume that the fault is located at z_f within the heterogenous slab, and its width is d_f . Its medium parameters are $\mu_f = 1$ and ϵ_f .

Thick faults: If the width of the fault is larger than the pulse width (i.e., $d_f > cT$) then its time-domain signature consists of the width d_f and of the contrast between its spectral characteristic impedance and the spectral characteristic impedance of the *ambient effective medium*. More explicitly, the last condition can be stated as $\sqrt{p_f/q_f} \neq \sqrt{p^{\text{ef}}/q^{\text{ef}}}$. In the numerical simulations, $z_f = 0.25$ and $d_f = 0.5$ with $\epsilon_f = \mu_f = 1$. The layered medium is the same medium considered in the previous examples, for which we find the effective parameters $\epsilon^{\text{ef}} \approx 2$ and $\mu^{\text{ef}} = 1$. For the pulse considered in the examples above we have $cT = 2^{-3}$ hence $c\sqrt{\epsilon^{\text{ef}}\mu^{\text{ef}}}T < d_f$ as required for monitoring the fault. Fig. 3 depicts the reflected pulse and one finds that the effective response agrees with the actual one for $\nu = 6$ but there are some differences for $\nu = 4$. Comparing these results with those shown in Fig. 1 for a layer without a fault, it is then possible to assess the fault properties (location and electrical width).

Thin faults: If the fault is very thin on the scale of the interrogating pulse (i.e. $d_f \ll cT$) such that it may be compared to the micro-scale heterogeneities, then it cannot be observed unless its contrast from the ambient multiscale heterogeneous medium is sufficiently large. The precise condition is determined by noting that a thin fault with high ϵ_f can be replaced with an impedance sheet and *surface admittance* $Y_s = -i\omega\epsilon_0\epsilon_f d_f$. The reflection coefficient is then estimated noting that a propagating short pulse, mainly feels the local characteristic admittance of the slowly varying effective medium $Y^{\text{ef}}(z) = \eta^{-1}\sqrt{p^{\text{ef}}(z)/q^{\text{ef}}(z)}$. The reflection coefficient becomes $\Gamma(\omega) = \frac{-Y_s}{Y_s + 2Y^{\text{ef}}(z_f)}$. In the limiting cases of $Y_s \gg Y^{\text{ef}}(z_f)$, we find that $\Gamma \approx -1$ or $\Gamma \approx \frac{i(\omega/c)\epsilon_f d_f}{\sqrt{q^{\text{ef}}(z_f)/p^{\text{ef}}(z_f)}}$, respectively. Thus, for small Y_s the reflected pulse is a derivative of the incident pulse while for large Y_s the reflected pulse essentially replicates the incident one. Furthermore, in order to sense the inclusion, the reflection coefficient should be non negligible, hence from the analysis above we have $\epsilon_f(d_f/cT) \gtrsim \sqrt{p^{\text{ef}}/q^{\text{ef}}}$.

In the numerical simulations we consider a thin layer at $z_f = 0.5$ and $d_f = 2^{-7}$, with $\mu_f = 1$ and $\epsilon_f = 20$. In Fig. 4 the reflected pulse is well observed, and the reflected waveform is essentially a derivative of the incident pulse. Note the excellent agreement between the actual and the effective solutions for $\nu = 6$, with certain discrepancies for the $\nu = 4$.

REFERENCES

- [1] B. Z. Steinberg, J. J. McCoy and M. Mirotznik, "A multiresolution approach to homogenization and effective modal analysis of complex boundary value problems," *SIAM J. Appl. Math.*, **60**(3), 939-966, March 2000.
- [2] V. Lomakin, B. Z. Steinberg and E. Heyman, "Multiresolution homogenization for radiation and propagation in multiscale laminates: Part I – Effective formulation," submitted for publication.
- [3] V. Lomakin, B. Z. Steinberg and E. Heyman, "Multiresolution homogenization for radiation and propagation in multiscale laminates: Part II – Spectral representations of the field," submitted for publication.
- [4] V. Lomakin, B. Z. Steinberg and E. Heyman, "UWB analysis of EM fields in complex laminates: An MRA homogenization approach," in *Ultra-Wideband, Short-pulse Electromagnetics*, **5**, P.D. Smith ed., Plenum Press, NY, 2001, in print.
- [5] I. Daubechies, *Ten Lectures on Wavelets*, CBMS–NSF Series in Applied Mathematics, SIAM Publ., Philadelphia, 1992.
- [6] C. E. Baum, "The Singularity Expansion Method," in *Transient electromagnetic fields*. L.B. Felsen, Ed. New York: Springer Berlag, 1976.

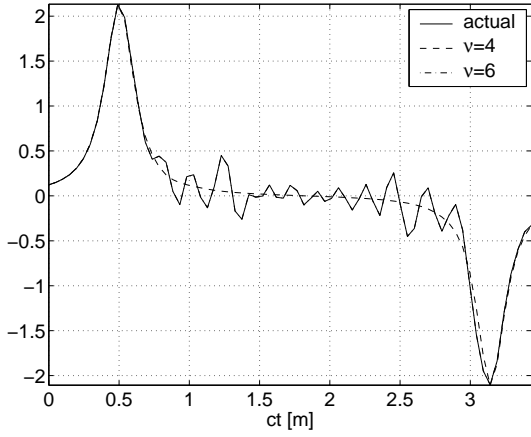


Figure 1: The transient reflected field calculated using the effective medium model, compared with the response of the actual heterogeneous laminate. The homogenization is performed using the non-dispersive approach for two values of the M-HS: $\nu = 4$ and 6 , with no noticeable difference between the response of the latter and of the actual medium

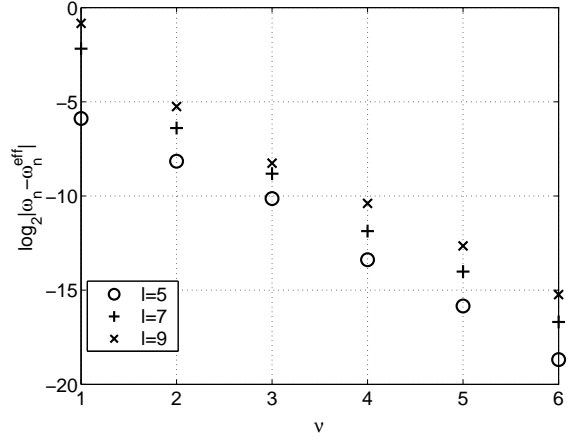


Figure 2: The error $|\omega_l - \omega_l^{\text{eff}}|$ in the SEM resonances, shown on a \log_2 scale as a function of the M-HS. The resonances plotted are $l = 5, 7$ and 9 . Note the excellent agreement with the parametric behaviour predicted in (4)

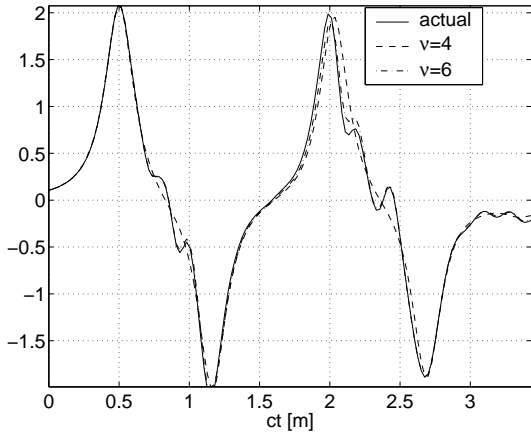


Figure 3: Pulse reflections from a heterogeneous laminate with a thick fault $d_f = 0.5$, $\varepsilon_f = 1$ at $z_f = 0.25$. Note the doublet-type pulse between $ct = 1.1$ and 2 , which is absent in the fault-free response of Fig. 1.

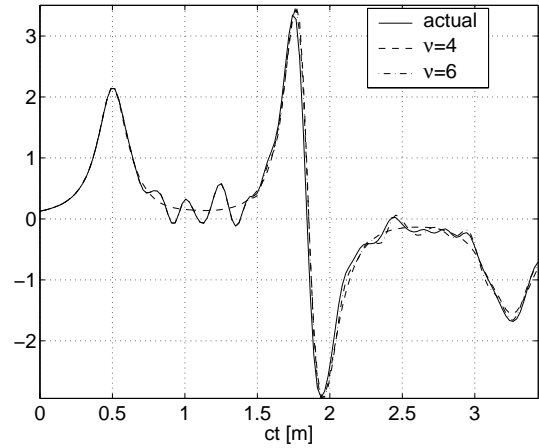


Figure 4: Pulse reflection from a heterogeneous laminate with a thin fault $d_f = 2^{-7}$ and $\varepsilon_f = 20$, at $z_f = 0.5$. Note the doublet-type pulse at $ct = 1.9$ which is absent in the fault-free response of Fig. 1.